THE LEADING EDGE
September 2007 Vol. 26, No. 9
Pages 91081-1232
Fractures

THE LEADING EDGE

September 2007, Vol. 26, No. 9

Special Section:
Fractures

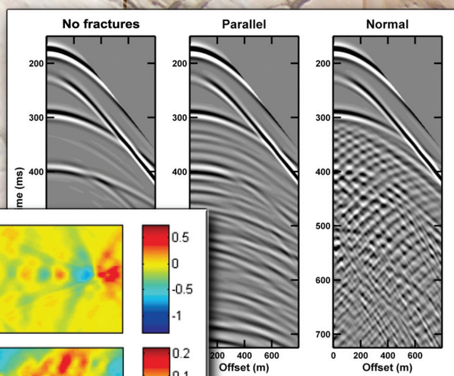

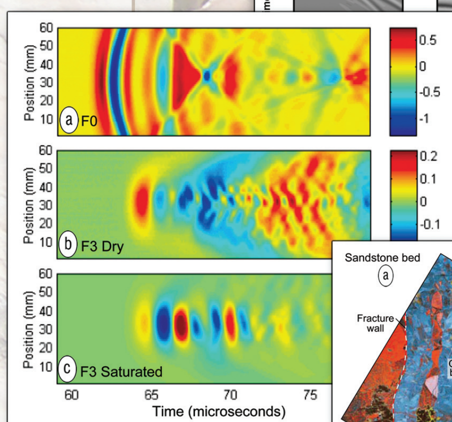

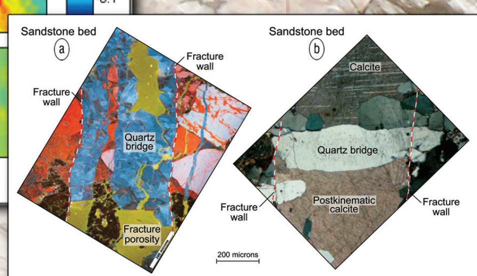

SEG
THE SOCIETY OF EXPLORATION GEOPHYSICISTS
The international society of applied geophysics
ISSN 1070-485X

Fracture anisotropy: The role of fracture-stiffness gradients

LAURA J. PYRAK-NOLTE, Purdue University, West Lafayette, Indiana, USA

Fractures in rock cause seismic anisotropy because they are oriented mechanical discontinuities that may occur in sets with preferred orientations. However, anisotropy from orientation can be altered or masked by gradients in stress and fluids. Such gradients in stress occur naturally in the Earth or are induced through anthropogenic activities. For instance, stress increases with depth in the Earth because of lithostatic forces, and in a given region, local gradients in horizontal stresses can arise through the tectonic history of the region (e.g., folding, faulting, etc.). In addition, gradients in fluid distributions as well as pore pressures occur when fluids are either injected or withdrawn from a rock formation.

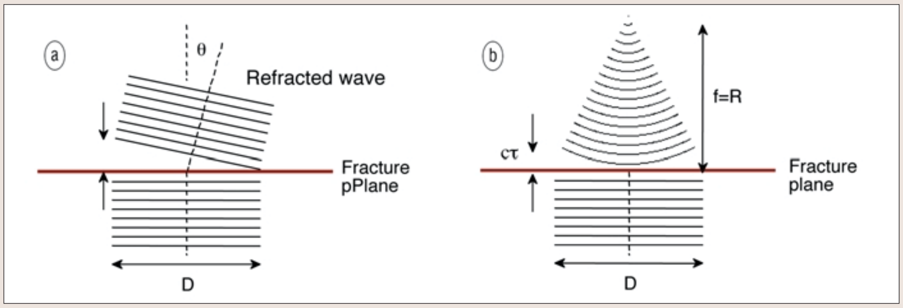

Figure 1. A fracture with (a) a linearly varying fracture-specific stiffness (high on the left to low on the right) and (b) a radially varying fracture-specific stiffness (low in the center and increases quadratically radially outward).

Gradients in stress are particularly significant for fractures because fractures are weakly coupled through the points of contact between the two fracture surfaces. This means that small physical modifications of the fracture can cause large changes in the mechanical, seismic, and hydraulic response of a fracture system. For instance, even low amounts of fluid saturation at the level of only 10% can double seismic transmission across a fracture. This occurs because the fluid provides a transmission medium around existing asperities, couple asperities, or it couples asperities across the fracture aperture. For such a weak-coupling system, the fracture geometry plays an essential role. The geometry defines not only the seismic properties of the fracture, but also the fluid flow through the fracture, which can be highly sensitive to stress. For example, the flow paths through the fracture are composed of the apertures and spatial distribution of regions of contacts that are sensitive to changes in stress. A factor of two decrease in aperture from an increase in stress on a fracture can lead to an order of magnitude decrease in the volumetric flow rate.

To understand these stress-induced changes on the fracture geometry, a useful quantity is fracture-specific stiffness. Stiffness relates the deformation of a fracture (closing apertures and increasing asperity contacts) to the stress. Stiff fractures displace less, while compliant fractures displace more. Theoretically, a fracture can be represented by a displacement discontinuity, i.e., stresses across the fracture are continuous but the displacements are not. The discontinuity in displacement is inversely proportional to the stiffness of the fracture. From experimental and numerical studies it has been shown that there is a general correlation of fracture geometry and fracture stiffness: compliant fractures tend to have larger apertures and fewer or smaller regions of contact than fractures that are stiffer. It is important to keep in mind that this correlation is statistical and not deterministic. Specific counter-examples certainly exist that show the opposite trend, but these special cases do not alter the average connection between fracture geometry and fracture stiffness.

The displacement-discontinuity theory has been used to derive plane-wave transmission and reflection coefficients for fractured media, group time delays, compressional-mode and Rayleigh-mode interface waves, guided Love waves, and dispersion relationships. Many of these studies have assumed that fracture stiffness is uniform along a fracture and uniform among fractures within a set. But, as described earlier, because stress gradients commonly exist or are induced in the Earth, one must consider what effects stress gradients have on seismic wave propagation in fractured media. Gradients in stress cause gradients in fracture-specific stiffness and ultimately affect any interpretation of seismic anisotropy.

If fracture-specific stiffness varies along a fracture, the time delay of a seismic wave also varies along the fracture plane. For example, consider a fracture with a linearly varying fracture-specific stiffness (Figure 1a) caused by a gradient in stress on the fracture. A plane wave propagating upward from below is refracted because the time-delay is a function of fracture-specific stiffness. A low fracture stiffness produces a larger time delay than a region of the fracture with high stiffness. While this refraction certainly violates Snell's law, it does not violate Fermat's principle of the path of least time.

An interesting example of the effect of stress gradient on seismic wave propagation across a fracture was studied by Oliger et al. (2003). They showed that a single plane fracture with an axially symmetric stress distribution (radial gradient in stress) behaves as a seismic lens that focuses seismic energy to a beam "waist" at a focal plane. A schematic of this concept is shown in Figure 1b. The fracture in Figure 1b has a stiffness that increases quadratically away from the center. The low stiffness in the center of the fracture delays the waves relative to the stiffness farther out along the fracture plane. For a wave propagating upwards from below, the wave is focused by the fracture. The location of the receiver in front of, at, or behind the focal plane determines whether a converging, planar, or diverging wave front is observed. Their work demonstrated that a 2D planar fracture with a stress gradient (contrasted with three-dimensional geologic structures such as basins and domes) can focus seismic waves. Focusing of seismic waves by fractures

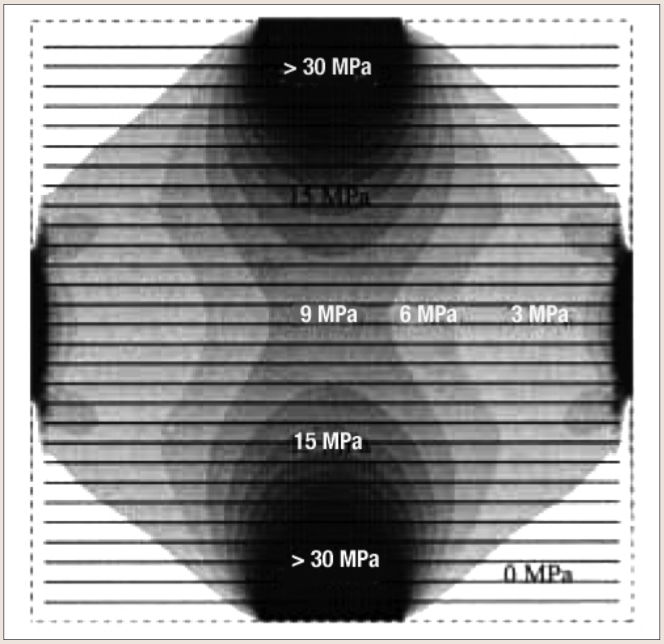

Figure 2. *The stress distribution (for stress component normal to the fracture plane) in a set of parallel fractures under bi-axial loading (after Hildyard and Young, 2002).*

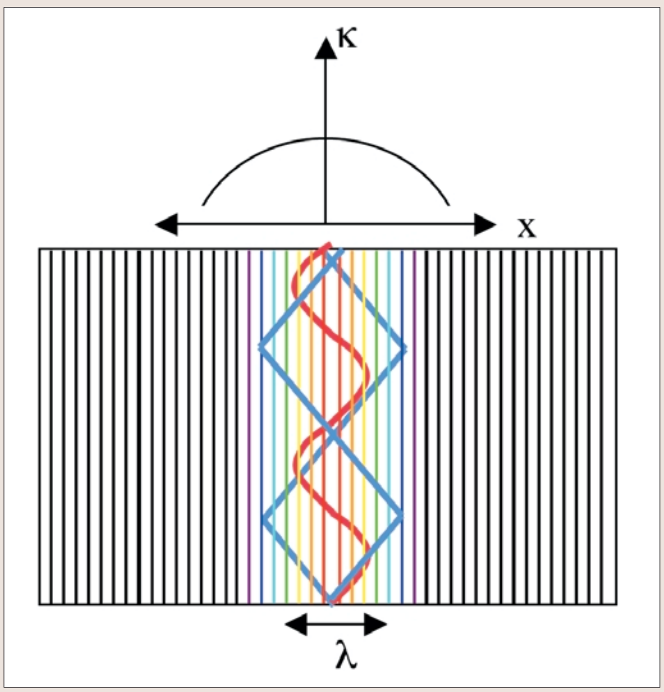

Figure 3. *A gradient in fracture stiffness (red=high stiffness decreasing to black=low fracture stiffness) among fractures in a set where the fracture spacing is much smaller than a wavelength.*

should be considered in the interpretation of seismic data from fractured strata with heterogeneous stress distributions.

Another example of the effect of stress gradients on the interpretation of seismic data from a set of parallel fractures can be found in Hildyard and Young (2002). They showed through a comparison of data and numerical modeling that knowledge of the state of stress in fractured systems is key for accurate interpretation of seismic data. In an attempt to reproduce, numerically, wave attenuation for shear and compressional waves propagated parallel or perpendicular to a set of parallel fractures, they found that stress distribution was of critical importance. Based on an analysis of the stress distribution in the experiment, the fracture-specific stiffness could not be assumed to be either the same among the fractures in the set, nor uniform along any single fracture within the set (Figure 2). In their analysis, the stress varied from 9 MPa to 30 MPa across the fracture set, and along the central fracture the stress varied from 3 MPa near the edges to 9 MPa in the center. By using a stress-dependent fracture-specific stiffness, they were able to match the laboratory data.

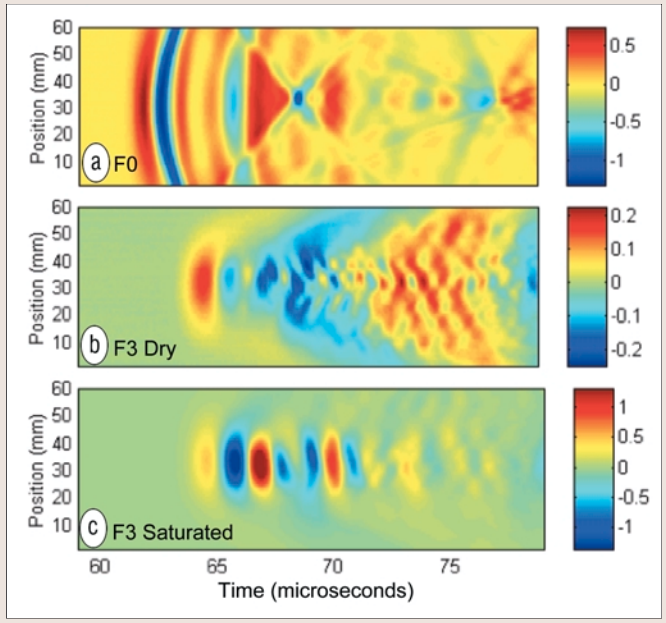

Figure 4. *Images of the acoustic wavefront propagated through (a) an intact sample F0, (b) fracture sample F3 in the dry condition, and (c) fracture sample F3 in the saturated condition. The fractures in the images for sample F3 are oriented parallel to the time axis and are spaced 3 mm apart (i.e., approximately 20 fractures occur between 0 and 60 mm). All of the wavefront images have a common time axis. The color scale on the right of each image represents the amplitude in volts. Note that the color scale is different for images (a), (b), and (c).*

While stress gradients can be eliminated or created in the laboratory through experimental design, stress distributions in the subsurface are set by lithostatic pressures, changes in pore pressure, as well as the local tectonic setting. Because wave attenuation and signal delay strongly depend on the stiffness of the fracture, gradients in stress certainly have significant consequences for the seismic interpretation of fracture properties in fractured reservoirs where the local stress field is perturbed during production.

Another strong fracture anisotropy arises when seismic waves are propagated parallel to fracture sets. Even when the fracture spacing is smaller than a wavelength, strong waveguiding can occur when the fracture-specific stiffness varies along the set. Figure 3 shows a set of parallel fractures with a fracture spacing much smaller than a wavelength where the fracture stiffness is high in the central fractures but decreases with distance from the center. This spatial variation in fracture-specific stiffness can produce waveguiding (as shown in Figure 3). Because of the gradients in stiffness, wave transmission across the fractures decreases and the waves become internally reflected within a group of fractures producing a wave guide. If the gradient in stiffness were similar to what is known in optics as a GRIN (graded index), the wave could snake though the layers.

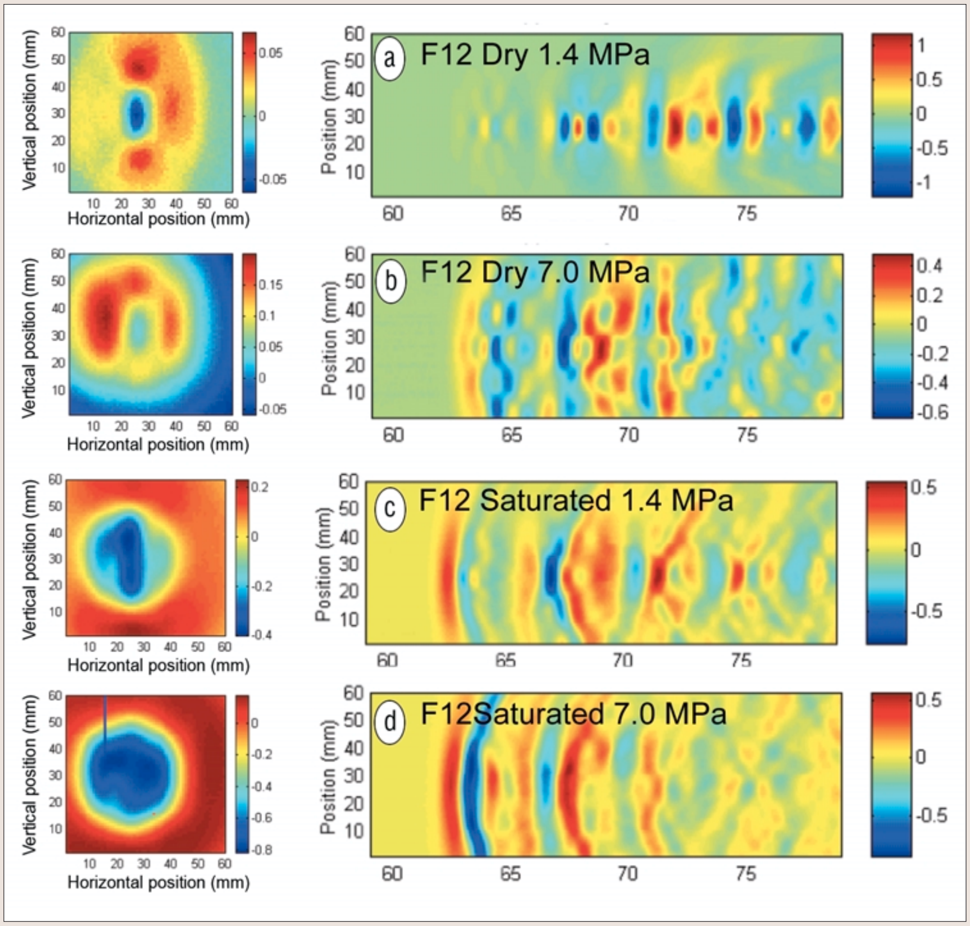

Figure 5. Acoustic wave front images are shown for fracture sample F12: (a) dry at 1.4 MPa, (b) dry at 7.0 MPa, (c) water-saturated at 1.4 MPa, and (d) water-saturated 7.0 MPa. The images on the left show the spatial distribution of energy for each condition taken at 63.5 microseconds. The images on the right represent a 20-microsecond window of the wavefront as a function of horizontal position (taken at a vertical position of 30 mm in the images on the left). The color scale associated with each image represents the amplitude in volts. Please note that the color scale is different for each image.

In a fracture system, energy confinement that spans several fractures is possible either with a stress-induced distribution of fracture-specific stiffness as shown in Figure 3 or with an uneven fluid saturation of fractures within a system of fractures. Water saturation increases both the normal and shear fracture-specific stiffnesses. As described earlier, a fracture can be viewed as being weakly coupled through the points of contact between the two surfaces. The addition of a fluid to this weakly coupled system significantly enhances the fracture stiffness. For normal stiffness, the coupling is enhanced through the bulk modulus of the fluid filling the fracture (e.g., water relative to air). For shear stiffness, the amount of enhancement is a function of the geometry of the fracture. For example, if the fracture surfaces are rough and interlocking, the void shapes might enhance shear-wave transmission (i.e., like a wet clutch). For smooth parallel surfaces, little enhancement in shear-wave transmission would be expected because shear waves decay in fluids. Thus, if a set of fractures were not uniformly saturated, a variation of both normal and shear fracture-specific stiffness can occur.

An example of waveguiding induced in a set of parallel fractures caused by uneven saturation within the set of fractures is given by Xian et al. (2001). They used wavefront imaging on aluminum samples with multiple parallel synthetic fractures to examine the effect of stress and saturation on wave propagation in a medium containing a set of parallel fractures. Aluminum samples were used, so all effects observed are the result of the factures and not of the background medium. Figure 4 shows the acoustic wavefront recorded for an intact reference sample, F0, and a fracture sample, F3. The fracture sample was composed of 28 fractures with a fracture spacing of 3 mm, a spacing that was roughly equal to a quarter of a wavelength at a frequency of 0.5 MHz. The intact sample exhibited a uniform wavefront (Figure 4a) because of the isotropy of the aluminum. On the other hand, for the dry fracture sample in Figure 4b, the first-arriving wavefront had a significantly smaller amplitude than the intact sample, and the waveform was mostly confined to within the central region spanning several fractures. There is a systematic trend in confinement as a function of frequency: the high-frequency components of the signal were the most strongly confined, while the dominant low-frequency energy was more weakly confined and had an earlier first arrival than the high-frequency components of the signal.

An anomalous behavior occurred when the fractures were exposed to water with the purpose of saturating the fractures. Because of trapped air in the fractures, the water saturation was incomplete. Furthermore, there were gradients in the fracture saturation across the set, which enhanced wave confinement rather than suppressing it. In the saturated condition (Figure 4c), the wavefront for the fracture sample was more strongly confined than the wavefront in the dry condition and was much larger in amplitude. This apparently anomalous behavior arose because the dominant low-frequency energy was confined by two fractures distant from the center of the sample, approximately at locations of 20 mm and 40 mm. The central fractures exhibited a larger value of stiffness than the fractures farther from the center, which confined the wave. These data illustrate that stiffness gradients in a set of parallel fractures can induce waveguiding even when the fracture spacing is much smaller than a wavelength. Interpretation of seismic data from fractured media would require both a knowledge of the local stress distribution as well as possible gradients in saturation.

Certainly, the opposite effect is more usually the case, in which saturation with water would be expected to decrease confinement anisotropy. As an example of this, Xian (2001) observed that a combination of stress and saturation could mask the presence of fractures. He used an aluminum fracture sample that had seven fractures with a fracture spacing equal to a wavelength (12 mm for a frequency of 0.5 MHz).

In Figure 5 (left), the fractures were oriented parallel to the vertical axis and were located at horizontal positions of approximately 6 mm, 18 mm, 30 mm, 42 mm, and 54 mm, and similarly for the right side of the figure.

The wavefronts for the dry fracture sample compared at low and high stresses (Figures 5a and b) show that increasing pressure on the sample decreased the confinement anisotropy. At low stress, the acoustic wavefront in the fracture sample was strongly confined to the central layer. For this sample, the source was located at about 26 mm on the horizontal axis and about 30 mm on the vertical axis. The acoustic wavefront was delayed by the fractures and spread out faster within the central confining layer than across the fractures. Energy confinement within the central layer was also observed in the image of the propagating wavefront (Figure 5a on the right). At this low stress, the low fracture-specific stiffness prevents any significant energy transmission across the fractures. The arrival time of the compressional mode wavefront is approximately the same as for the intact sample (Figure 4a) while the wavefronts outside the central waveguide are delayed and attenuated by each fracture that the wavefront crosses.

On the other hand, at high stress (Figure 5b), the increased fracture-specific stiffness allows greater transmission of energy across the fractures, less delay of the wavefront, and less energy confinement in the central layer between fractures. The nonsymmetry in the amplitude in the image of the acoustic wavefront (Figures 5a and b) also indicates that the fracture-specific stiffness for each fracture, and even for different locations on the same fracture, were not equal. For example, Figure 5b shows that the fracture at a horizontal position of 30 mm had a different stiffness than the fracture at a horizontal position of 18 mm based on the asymmetry of the wavefront. Thus, symmetric positions in the wavefront relative to the central layer do not have the same energy.

Homogeneous saturation of the fractures with water, combined with high stress, removes the strong effect of fractures on the acoustic wavefront and makes the fractures nearly invisible. By comparing Figures 5a and 5c (or Figures 5b and 5d) for the same confining pressure, more energy is propagated across the saturated fractures than across the dry fractures. Increasing the stiffness of a fracture further increases the transmission of energy across the fracture and reduces the amount of energy that is internally reflected into a guided mode. At a confining pressure of 7.0 MPa for the saturated condition (Figure 5d), the first-arriving wavefront is nearly uniform and the presence of fractures is only observed in the later arrivals. The wavefront exhibited a slight ellipticity (Figure 5d on the left), although the high stiffnesses of the fractures enabled the wavefront to spread out almost as if there were no fractures. The energy distribution was observed to be roughly symmetric and only a slight delay in the wavefront occurred as it propagated across the fractures. This demonstrates that seismic anisotropy caused by parallel sets of fractures can be masked by saturating the fractures with a liquid. Hence, application of both stress and fluid saturation (homogeneously) essentially erases the effects of the fractures on a propagating wavefront.

In summary, I have shown that the ability to interpret fracture properties from seismic data is linked to spatial variations in fracture-specific stiffness. Several examples of the effect of gradients in fracture-specific stiffness on seismic wave propagation were presented to convey a sense that gradients in fracture-specific stiffness play an important role in seismic anisotropy caused by fractures. Fracture-specific stiffness is intimately linked to the many different length scales associated with fracture geometry (apertures, spatial correlations, contact area, etc.) and to how these length scales are altered through physical processes. The length scales associated with the examples given in this paper are much smaller than those encountered in the field. However, an understanding of length scales associated with fractures and fracture sets relative to seismic length scales is relevant because it determines when a fractured medium can be treated as an effective medium, or when a discrete fracture approach is necessary. In addition, it is important to recognize that physical processes (such as stress, fluids, etc.) can either homogenize a fracture stiffness, or it can induce greater complexity within a fracture or among fractures within a set. Therefore, a system that initially may be represented as an effective medium may fail to be so as alterations to a fractured reservoir proceed, and vice versa. A fundamental understanding of how gradients in fracture-specific stiffness alter the seismic response of a fractured medium will help improve the interpretation of seismic data and to recognize deviations from homogeneity.

Suggested reading. "Modeling seismic waves around underground openings in fractured rock" by Hildyard and Young (*Pure and Applied Geophysics*, 2002). "Focusing of seismic waves by a single fracture" by Oliger et al. (*Geophysical Research Letters*, 2003). "Transmission of seismic waves across single natural fractures" by Pyrak-Nolte et al. (*Journal of Geophysical Research*, 1990). "Single fractures under normal stress: The relation between fracture-specific stiffness and fluid flow" by Pyrak-Nolte and Morris (*International Journal of Rock Mechanics and Mining Sciences*, 2000). "Compressional waves guided between parallel fractures" by Xian et al. (*International Journal of Rock Mechanics and Mining Sciences*, 2001). "Wavefront imaging of energy confinement by multiple parallel fractures" by Xian (MS thesis, Purdue University, 2001). TLE

Acknowledgments: The author acknowledges support of this work by the Geosciences Research Program, Office of Basic Energy Sciences, U.S. Department of Energy (DE-FG02-97ER14785 08).

Corresponding author: ljpn@physics.purdue.edu